Atmospheric
Chemistry
and Physics
Discussions

Open Access

Impacts of new particle formation on aerosol cloud condensation nuclei (CCN) activity in Shanghai: case study

C. Leng[1], Q. Zhang[1], D. Zhang[1], H. Zhang[2], C. Xu[1], X. Li[1], L. Kong[1], J. Tao[3], T. Cheng[1], R. Zhang[4], J. Chen[1], L. Qiao[5], S. Lou[5], H. Wang[5], and C. Chen[5]

[1]Shanghai Key Laboratory of Atmospheric Particle Pollution and Prevention (LAP[3]), Fudan-Tyndall Centre, Department of environmental science and engineering, Fudan University, Shanghai 200433, China
[2]Atmospheric Environment Institute, Chinese Research Academy of Environmental Sciences, Beijing 100012, China
[3]South China Institute of Environmental Sciences, Ministry of Environmental Protection, Guangzhou 510655, China
[4]Key Laboratory of Region Climate-Environment Research for Temperate East Asia, Institute of Atmospheric Physics, Chinese Academy of Sciences, Beijing 100029, China
[5]State Environmental Protection Key Laboratory of the Cause and Prevention of Urban Pollution Complex, Shanghai Academy of Environmental Sciences, Shanghai 200233, China

ACPD

14, 18641–18677, 2014

Impacts of new particle formation on aerosol CCN

C. Leng et al.

Title Page

Abstract | Introduction

Conclusions | References

Tables | Figures

|◄ | ►|

◄ | ►

Back | Close

Full Screen / Esc

Printer-friendly Version

Interactive Discussion

Impacts of new particle formation on aerosol CCN

C. Leng et al.

Title Page

Abstract | Introduction

Conclusions | References

Tables | Figures

◄ | ►

◄ | ►

Back | Close

Full Screen / Esc

Printer-friendly Version

Interactive Discussion

Abstract

New particle formation (NPF) events and their impacts on cloud condensation nuclei (CCN) were investigated using continuous measurements collected in urban Shanghai from 1 to 30 April 2012. During the campaign, NPF occurred in 8 out of the 30 days and enhanced CCN number concentration (N_{CCN}) by a factor of 1.2–1.8, depending on supersaturation (SS). The NPF event on 3 April 2012 was chosen as an example to investigate the NPF influence on CCN activity. In this NPF event, secondary aerosols were produced continuously and increased PM$_{2.5}$ mass concentration at a rate of $4.33\,\mu g\,cm^{-3}\,h^{-1}$, and the growth rate (GR) and formation rate (FR) were on average $5\,nm\,h^{-1}$ and $0.36\,cm^{-3}\,s^{-1}$, respectively. The newly formed particles grew quickly from nucleation mode (10–20 nm) into CCN size range. N_{CCN} increased rapidly at SS of 0.4–1.0 % but weakly at SS of 0.2 %. Correspondingly, aerosol CCN activities (fractions of activated aerosol particles in total aerosols, N_{CCN}/N_{CN}) were significantly enhanced from 0.24–0.60 to 0.30–0.91 at SS of 0.2–1.0 % due to the NPF. On the basis of the κ-Köhler theory, aerosol size distributions and chemical composition measured simultaneously were used to predict N_{CCN}. There was a good agreement between the predicted and measured N_{CCN} ($R^2 = 0.96$, $N_{predicted}/N_{measured} = 1.04$). This study reveals that NPF exerts large impacts on aerosol particle abundance and size spectra, thus significantly promotes N_{CCN} and aerosol CCN activity in this urban environment. The GR of NPF is the key factor controlling the newly formed particles to become CCN at all SS levels, whereas the FR is an effective factor only under high SS (e.g. 1.0 %) conditions.

1   Introduction

Atmospheric aerosols exert great impacts on global climate by affecting the earth's radiation balance through directly scattering and absorbing solar and terrestrial lights, and indirectly modifying cloud by acting as cloud condensation nuclei (CCN) (Charl-

son et al., 1992; Lohmann et al., 2005). The indirect effect of primary and secondary aerosols brings up the largest uncertainty to predictions of aerosol radiative forcing and global climate change (IPCC, 2013). So far, many studies of field observation and modeling have found that new particle formation (NPF) significantly impacts aerosols and CCNs at worldwide locations (Ghan et al., 2001; Spracklen et al., 2006, 2008; Zhang et al., 2010).

Normally, NPF in the atmosphere is identified as the nucleation of gas phase precursors and subsequent condensational growth, which is a crucial secondary transformation course (Birmili et al., 2000; Kulmala et al., 2004). In fact, NPF consists of a complex set of procedures, including the formation of nanometer-size clusters from gaseous vapors, the growth of these clusters, the removal of growing clusters by coagulation with pre-existing particles, and the further growth of survived clusters into aerosol particles, some of which are large enough to become CCN (McMurry et al., 1983, 2005; Weber et al., 1996). The NPF event can be effectively characterized by the formation rate (FR) of nucleation mode particles and the growth rate (GR) of freshly nucleated particles (Kulmala et al., 2012). On the basis of over 100 field measurements summarized by Wang et al. (2013), significant gaps still exist regarding both formation and growth rate outputs. For example, the GR varied in the range of 1–$20\,\mathrm{nm\,h^{-1}}$ and the FR in 0.01–$10\,\mathrm{cm^{-3}\,s^{-1}}$. Condensable gaseous precursors and their coagulation sink responsible for NPF are commonly high in megacities of developing countries (Mönkkönen et al., 2005; Wu et al., 2007). Gaseous sulfur is proved to play a vital role in nucleation process (Petäjä et al., 2009; Kulmala et al., 2013), and atmospheric ammonia participates homogeneous nucleation with gaseous sulfur acid and water vapor because of significantly low surface pressure of gaseous sulfuric acid molecular (Smith et al., 2004; Sakurai et al., 2005; Gaydos et al., 2005). In addition, there are other species responsible for NPF such as amines (Yu et al., 2012; Benson et al., 2011), low-volatile organic vapors (Metzger et al., 2010; Paasonen et al., 2010; Riipinen et al., 2011; Ehn et al., 2014) and iodine compounds (O'Dowd et al., 2002; Vuollekoski et al., 2009).

The newly formed particles from atmospheric nucleation are often able to grow into CCN size and further influence cloud properties or even global climate (Kerminen et al., 2005; Laaksonen et al., 2005; Wiedensohler et al., 2009). Kerminen et al. (2012) presents a synthesis of our current (by the end of 2012) knowledge of CCN production associated with atmospheric nucleation, and concludes that CCN production associated with atmospheric nucleation is both frequent and widespread phenomenon in numerous types of continental boundary layers, and probably also for a large fraction of the free troposphere. The latest model results show that the NPF events contribute much more to global aerosol number burden than primary emissions (Merikanto et al., 2009; Yu et al., 2008). Under numerous atmospheric conditions aerosol has a positive feedback to CCN number concentration (N_{CCN}) (Ramanathan et al., 2001; Laaksonen et al., 2005), and N_{CCN} usually exhibits a significant increase after NPF (O'Dowd et al., 2001; Lihavainen et al., 2003; Kuwata et al., 2008; Yue et al., 2011). Due to various chemical species involved in NPF, the extent of NPF effects on CCN varied temporarily and spatially (Spracklen et al., 2008; Pierce and Adams, 2009). The long-term NPF observations were mainly conducted in Europe and North America, whereas little has been done in developing countries (Wang et al., 2013). To date, only a few studies have concerned NPF and its interaction with CCN in China. Yue et al. (2011) reported that the GR of sulfur-poor NPF was on average about 80 % larger than that of sulfur-rich NPF, and the NPF events increased CCN by 0.4–6 times in Beijing, where various source apportionment of $PM_{2.5}$ was reported by Zhang et al. (2013). Wiedensohler et al. (2009) found that the CCN size distribution is dominated by the growing nucleation mode in Beijing, which accounted up to 80 % of the total CCN number concentration, in contrast to the usually found phenomenon of the dominance by the accumulation mode.

In the present study, we analyze a comprehensive dataset of 1 month simultaneous measurements of aerosol size spectra, N_{CCN}, black carbon (BC), water-soluble ions and gaseous pollutants to understand the NPF events and their impacts on N_{CCN} and aerosol CCN activity in an urban environment of Shanghai, one of the largest cities

in China. A closure study between predicted and measured CCNs is also conducted to investigate the influence of aerosol chemical composition on its growth to CCN. An effective CCN prediction model is further developed based on model-measurement comparison results.

2 Experimental

2.1 Observational site

All instruments were mounted on the roof of one building approximately 20 m above the ground in the campus of Fudan University (31°18′ N, 121°29′ E) located in Shanghai. The observational site is mainly surrounded by urban residential areas, where no large local emission was detected during this study. The East China Sea is approximate 40 km east of the site. Except CCN, other measurements conducted synchronously, including aerosol number size distribution (condensation nuclei (CN) of 10–800 nm), major inorganic water-soluble ions in aerosol particles, gaseous pollutants and meteorological factors. Local time (LT) used in this study is eight hours ahead of UTC.

2.2 Measurement and instrumentation

A CCN counter (CCN-100, DMT, USA) with continuous flow and single column (Roberts and Nenes, 2006; Lance et al., 2006) was employed to monitor CCN concentrations at supersaturated conditions (SS in the range of 0.07–2 %). Before the campaign, the instrument was calibrated for SS using standard $(NH_4)_2SO_4$ particles. To maintain stable SS, according to the instrument operation manual, regular calibrations were also performed for temperature gradient, input and shear airflows and pressure (Leng et al., 2013). In addition, periodic zero checks were done to ensure counting accuracy for optical particle counter (OPC) installed inside the CCN counter. The ambient aerosol was firstly dried by a dryer (active carbon) to lower relative humidity (RH) below 30 %, and subsequently introduced into the CCN counter (Leng et al., 2013).

Aerosol particle size distributions in the size range of 10–800 nm were measured using a high-resolution scanning mobility particle sizer (SMPS, TSI 3080, USA). Before and after the field campaign, the instrument was calibrated to maintain accurate particle sizing.

BC was measured by an online monitor of Aethalometer (AE-31, Magee Scientific Co., Berkeley, California, USA) at a 5 min time resolution and a $5 \, L \, min^{-1}$ airflow rate. According to the strong ability of BC light absorption at near infrared wavelengths (Hansen et al., 1984; Weingartner et al., 2003), BC mass is determined using the light attenuation at 880 nm and the appropriate specific attenuation cross section proportional to BC (Petzold et al., 1997). The attenuation can be calculated based on the intensity difference of reference and sensing beams between light on and off (Dumka et al., 2010). In order to screen the impacts of other absorptive material, the data contaminated by mineral and dust aerosols were excluded from BC measurements. Details for instrument operating and calibrating can be found in Cheng et al. (2010).

A monitor of aerosols and gases (MARGA, ADI 2080, Netherlands) was employed to measure the mass concentrations of major inorganic water-soluble ions (Na^+, K^+, Mg^+, Ca^+, SO_4^{2-}, Cl^-, NO_3^- and NH_4^+) in ambient aerosol particles at a 1 h time resolution. The methods of sampling, operation and internal calibration of the MARGA were described in Du et al. (2011).

Moreover, a continuous ambient particulate monitor (FH62C14, Thermo) was used to measure $PM_{2.5}$ (particles in aerodynamic diameter less than 2.5 μm) concentration online. An automatic weather station client (HydroMet^{TM}, Vaisala) and a visibility monitor (Vaisala) were employed to collect the data of meteorological variables and atmospheric visibility.

3 Results and discussion

3.1 Overview of the entire period

The ground-based measurements contained N_{CCN} at SS of 0.2–1.0 %, aerosol size spectra, atmospheric visibility, $PM_{2.5}$, BC, aerosol inorganic water-soluble ions and SO_2 and were conducted during the period of 1–30 April 2012. Figure 1 describes the general meteorological conditions (e.g. wind speed, wind direction, RH and temperature) for the entire period. Wind frequently changed direction and were mostly weaker than $6\,\mathrm{m\,s}^{-1}$. There was no significant precipitation in this month and RH seldom exceeded 90 %. Temperature generally varied between 10–25 °C.

Figure 2 shows the temporal variations of 5 min mean SO_2, $PM_{2.5}$ concentration and atmospheric visibility for the entire period. In general, $PM_{2.5}$ and visibility were negatively correlated and averaged $70 \pm 60\,\mu\mathrm{g\,m}^{-3}$ and $24.3 \pm 23.7\,\mathrm{km}$, respectively. The maximum and average of $PM_{2.5}$ in the current study is of less magnitude than those measured in a previous study in 2006 in this urban environment which showed a range of $17.8–217.9\,\mu\mathrm{g\,m}^{-3}$ and an average of $94.6\,\mu\mathrm{g\,m}^{-3}$ (Wang et al., 2006). $PM_{2.5}$ frequently experienced a clear inter-day oscillating with a similar intra-day cycle. $PM_{2.5}$ can reflect the variations of ambient particulate pollutant loadings in the boundary atmosphere layer, and can be viewed as an additional proxy of pre-existing particle amounts for identifying NPF. In a broad view, atmospheric visibility frequently declined to be less than 10 km, revealing heavily polluted episode occurrences (e.g. haze). In fact, the haze or hazy days accounted for 50 % of the study period, during which atmospheric visibility was on average 5.65 km, while it was 24.3 km on average for the rest of the days.

3.1.1 New particle formation event

It has been widely accepted that the key criterion for discerning an NPF event is to identify an acute burst of nucleation mode particles, known as newly formed particles

up to detectable size of 3 nm exceeding the background level and lasting for several hours and subsequent growth in mean particle size (Birmili and Wiedensohler, 2000; Kulmala et al., 2004, 2012; Vakkari et al., 2011). The supplementary criterions are also needed for identifying NPF, such as low pre-existing particle loading, an apparent "banana" shaped particle number concentration as a function of time and size, and favorable weather conditions essential for excluding pre-existing particle disturbance particularly in urban environment (Shi et al., 2001; Heintzenberg et al., 2007; Olofson et al., 2009). In this study, although the SMPS is only capable of capturing particles no less than 10 nm, the aerosol size spectra from the SMPS measurements was available to determine NPF and to calculate the FR and GR of NPF.

In this study, the days with distinct bursts of nucleation mode (10–20 nm) particles lasting for at least 1.5 h from their initial outbreak to maximum in number concentration, and with apparent growth to larger sizes (e.g. 20–50 nm) for a few hours, were defined as effective NPF days. The rest of the days were defined as non-NPF days. Figure 3 shows the 1 month series of aerosol size distribution, 5 min mean total (N_{total}) and nucleation mode ($N_{\text{10–20 nm}}$) aerosol number concentration and 1 h mean CCN concentration. On a whole, 8 out of the 30 days were characterized as the NPF days, which represented an occurrence frequency of 27 % and was much higher than the 5.4 % measured by Du et al. (2012) at the same site in winter.

3.1.2 Formation and growth rate

Formation and growth rates are two essential factors characterizing NPF events (Yue et al., 2011; Kulmala et al., 2012). The FR rate is theoretically defined as the mean increase rate of nucleation mode particle in number concentration as a function of time ($dN_{\text{nucleation}}/dt$) during the nucleation stage of a NPF event. In this paper, due to the losses of newly-formed nucleated particles caused by coagulation, and the measurement unavailable for 3–10 nm particles, this calculation only yielded an "apparent particle formation rate (APFR)" (Du et al., 2012). It should be noted that this APFR would be an underestimate in comparison with the actual FR rate. On the other hand, the

GR rate refers to the mean size growing rate of nucleated particles in geometric mean diameter as a function of time during the growth stage of a NPF event, which has been described in details elsewhere (Kulmala et al., 2001, 2004b; Dal Masol et al., 2005). The mode diameter, namely a calibrated geometric mean diameter automatically made by SMPS itself for all aerosol size bins instead of only for nucleated particles, is used to calculate particle growth rate in this study. Similarly, this calculation produces an "apparent particle growth rate (APGR)". The APGR would be an overestimate in comparison with the real GR rate due to inclusion of the GR rate caused by coagulation, which is not related to particle mass increases (Kerminen and Kulmala, 2002).

The mean FR and GR rates of NPF events were $0.40\,\mathrm{cm^{-3}\,s^{-1}}$ and $4.91\,\mathrm{nm\,h^{-1}}$, respectively, during the whole campaign. The FR and GR rates showed a strong location dependence, for example, higher FR and GR have been observed in New Delhi (3.3–$13.9\,\mathrm{cm^{-3}\,s^{-1}}$, 11.6–$18.1\,\mathrm{nm\,h^{-1}}$) and Atlanta ($20$–$70\,\mathrm{cm^{-3}\,s^{-1}}$), while comparable FR was measured in Beijing ($6\,\mathrm{cm^{-3}\,s^{-1}}$, $4\,\mathrm{nm\,h^{-1}}$) for sulfur-rich aerosol type and ($2\,\mathrm{cm^{-3}\,s^{-1}}$, $6\,\mathrm{nm\,h^{-1}}$) for sulfur-poor aerosol type and in Shanghai (3.3–$5.5\,\mathrm{nm\,h^{-1}}$) (Kulmala et al., 2004; Mönkkönen et al., 2005; Yue et al., 2011; Du et al., 2012).

3.1.3 NPF impacts on aerosol CCN activity

Pierce and Adams (2007) are the first ones that present the full theoretical framework on the efficiency of CCN production resulting from nucleation. To explore the NPF potential influence on CCN, we further examined the impacts of FR and GR rates in NPF events on N_{CCN} and aerosol CCN activity. Table 1 summarizes the N_{CCN} enhancement ratios for different FR and GR levels during the entire campaign.

It has been widely recognized that N_{CCN} is positively correlated to N_{CN} under various atmospheric conditions (Ramanathan et al., 2001; Laaksonen et al., 2005), and enhancements on N_{CCN} are expected after NPF events (O'Dowd et al., 2001; Kuang et al., 2009; Yue et al., 2011). Theoretically, the high FR rate produces more secondary aerosol particles (i.e. N_{CN}), which may subsequently impact N_{CCN} if new particles grow into greater sizes (Ghan et al., 2001; Spracklen et al., 2006, 2008; Zhang et al., 2010).

In this paper, however, N_{CCN} was insensitive to the FR rate of NPF at SS of 0.2–0.8 %, as indicated by the small differences in N_{CCN} enhancement ratios under various FR and SS values. This finding agrees with the results of earlier studies that the nucleation of newly formed particles within the boundary layer poses a minor impact on N_{CCN}. Carslaw et al. (2007) found that N_{CCN} increased only by 12–17 % after a two order of magnitude increase of nucleation rate in central Europe. A similar result has been reported in Beijing (Yue et al., 2011). The possible explanation is in two aspects. The first one is due to the two separate and self-governed processes in particle formation and subsequent growth. A high formation rate does not necessarily correspond to a high GR rate since the newly formed particles may not grow into CCN size with insufficient time period. The second one is due to coagulation process between particles which leads to reduced N_{CN} and further lowers N_{CCN} enhancement ratios. In fact, the impact of FR in NPF on N_{CCN} enhancement increased with SS (Table 1). The lower critical dry diameter under higher SS for a given aerosol particle was probably the main reason. For example, according to the κ-Köhler theory (Köhler, 1936; Petters and Kreidenweis, 2007), pure NaCl particles can act as CCN only at 65 nm under SS 0.2 %, while it can be activated at 22 nm under SS 1.0 %. Presumably, with the presence of an unrealistic high SS where all nucleation mode particles (10–20 nm) are activated, the formation rate would be one controlling factor.

On the other hand, what controls a newly formed particle to become a CCN is its survival probability whether it has enough time to grow into thermodynamic stable size by competing with the capture and removal of pre-existing particles (Kerminen et al., 2001; Pierce and Adams, 2007; Zhang et al., 2012). Toward to this end, the aerosol GR rate of NPF responsible for this survival probability was observed to exert a valid effect on N_{CCN} enhancement ratios. As was found in this study, the N_{CCN} enhancement ratios at larger GR rate were higher than those at lower GR rate by a factor of 1.06–1.13 depending on SS.

Overall, the N_{CCN} enhancement ratios due to NPF varied as a function of FR and GR rates and SS. In real atmosphere, SS varys from exceeding 1.0 % in clean-air stratus

cloud to slightly less than 0.1 % in polluted conditions (Hudson and Noble, 2014). FR may logically play a vital role in CCN production in the clean-air stratus cloud while exert a minor impact in polluted conditions. GR is invariably the most important factor in controlling the extent of newly formed particles in becoming CCN during NPF.

3.2 Characteristics of the typical NPF

3.2.1 Enhancement of nanoparticles

The NPF event spanning the period from 10:00 LT on 3 April to 04:00 LT on 4 April is analyzed in detail to shed some light on the relationship between NPF and CCN. This NPF event was identified to consist a nucleation stage (10:00–13:00 LT) and a growth (13:00–04:00 LT) stage (Fig. 4).

Before 10:00 LT on 3 April, $PM_{2.5}$ was below $20\,\mu g\,m^{-3}$ due to the relatively strong wind speed (e.g. $6\,m\,s^{-1}$) favoring pollutant dispersion. BC was less than $1\,\mu g\,m^{-3}$ and atmospheric visibility exceeded 30 km (Figs. 5 and 6). Apparently, the pre-existing particles of nucleation mode (10–20 nm) were low (Fig. 7). Newly formed particles increased quickly in just 1.5 h from the initial outbreak to the maximum concentration of $1800\,cm^{-3}$ (Fig. 7). During the same time period, N_{CN} increased from 15 000 to $25\,000\,cm^{-3}$. The newly formed particles grew in size in the following periods (the growth stage) due to condensation, heterogeneous reactions of chemical compounds and coagulation between particles (Wang et al., 2010). The temporal variations of median, geometric mean and mode diameters for the measured aerosol population are given in Fig. 7. In general, these three diameters were strongly correlated with each other and increased in size ever since the nucleation burst occurred. During this period, the wind speed was mostly less than $2\,m\,s^{-1}$, implying a weak atmospheric dilution of pollutants. $PM_{2.5}$ increased after 17:00 LT on 3 April, showing a significant enhancement from 38 to $86\,\mu g\,m^{-3}$. In addition, BC correlated well with $PM_{2.5}$, and they both reduce atmospheric visibility.

3.2.2 Insights into chemical species involved

Several factors likely determine if a chemical species is to act as nucleation precursor, including its abundance, reactivity and volatility (Zhang et al., 2012). Gaseous H_2SO_4 has been proved to be a key precursor participating in nucleation process due to its low volatility (Petäjä et al., 2009; Kulmala et al., 2013), and a necessary condition for new particle formation is for its molecular concentration exceeding 10^5 cm^{-3} in atmosphere (Weber et al., 1999; Nieminen et al., 2009). The condensation of gaseous H_2SO_4 together with subsequent neutralization with ammonia plays a dominant role in the growth of Aitken mode particles, whereas it exerts little contribution to the growth of particles in accumulation mode (Zheng et al., 2011).

However, direct measurement of sulfuric acid in ambient air is still challenging, appropriate proxies are needed. Petäjä et al. (2009) measured the sulfuric acid and OH concentration in a boreal forest site in Finland and successfully developed three reasonable proxies for sulfuric acid concentration by using the measured time series as a foundation. Their proxies refer to source (i.e. gaseous SO_2, hydroxyl radical, solar radiation in 280–320 nm range, and global radiation) and sink (i.e. condensation sink) terms, and the simplest one is the radiation times SO_2 divided by condensation sink. In this paper, the source and radiation terms are unavailable, one may plausibly conjecture similar promotion of H_2SO_4 on the basis of its gaseous precursor (e.g. SO_2) evolution (Zhang et al., 2012).

$$SO_2 + OH \xrightarrow{O_2H_2O} H_2SO_4$$
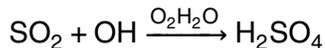
The particle nucleation event showed a burst of 10–20 nm particles when SO_2 peaked at 10:00 LT on 3 April, with its mass and molar concentrations exceeding 4.1 µg m^{-3} and 3.8×10^{10} cm^{-3}, respectively (Fig. 8). Afterwards, SO_2 underwent a gradual decrease down to 1.5 µg m^{-3}, and SO_4^{2-} correspondingly increased from 8 to 10 µg m^{-3}. The good agreement between SO_2 and nucleation mode particles denotes

Discussion Paper | Discussion Paper | Discussion Paper | Discussion Paper

the key role of gaseous sulfur in controlling particle nucleation (Kulmala et al., 2013; Zhang et al., 2012).

Besides gaseous sulfur, other nucleation precursors have been proposed to involve in the critical nucleus formation in numerous environment conditions (Zhang et al., 2012; Riipinen et al., 2011). For example, atmospheric ammonia can significantly lower the surface vapor pressure of gaseous sulfuric acid molecular and participate homogeneous nucleation with gaseous sulfur acid and water vapor. According to the classical ternary homogeneous theory developed recently, the presence of ammonia in ppt level significantly enhances nucleation rates (Yu et al., 2006). Many field measurements and laboratory simulations have corroborated the crucial role of ammonia in the growth of newly formed particles (Smith et al., 2004; Sakurai et al., 2005; Gaydos et al., 2005). Though experimental evidence seems very limited, nitrate has been reported as a crucial contributor to nanoparticle growth, especially for 10–30 nm particles where nitrate is dominant (Hildebrandt et al., 2012). Riipinen et al. (2011) combined observations from two continental sites to show that condensation of organic vapors (i.e. non-volatile and semi-volatile species) is a crucial factor governing the lifetimes and climatic importance of the smallest atmospheric particles. Ehn et al. (2014) find that several biogenic VOCs (e.g. monoterpenes) form large amounts of extremely low-volatility vapours and further demonstrate that these low-volatility vapours can enhance (or even dominate) the formation and growth of aerosol particles over forested regions. In this paper, NO_3^- increased by a factor of 1.33 and NH_4^+ increased by a factor of 1.45 during the case NPF event, indicating that the particle growth is partly driven by the condensation of atmospheric precursors (Fig. 8).

3.2.3 Aerosol CCN activity enhancement

Figure 9 shows the temporal evolutions of N_{CCN} and aerosol CCN activity at SS of 0.2–1.0 % for the entire period. The enhanced N_{CN} and reduced aerosol CCN activity, associated with nucleation mode particle burst, was observed between 10:00 and 13:00 LT on 3 April. In contrast to N_{CN} which increased immediately after the burst of nucleation

mode particles, there was a 4 h delay in the increase of N_{CCN}. As the newly formed particles grew into larger sizes, both N_{CCN} and aerosol CCN activity increased at various stages under different SS. At a SS higher than 0.4 %, N_{CCN} peaked at 20:00 LT on 3 April. N_{CCN} greatly promoted from 8000–12 000 cm^{-3} to 13 000–20 000 cm^{-3} under higher SS, however, only slightly from 6000 to 7000 cm^{-3} under lower SS (e.g. 0.2 %). Larger critical dry diameter corresponding to lower SS should be the main reason. For example, the critical dry diameter for pure $(NH_4)_2SO_4$ particle was 83 nm at SS of 0.2 % and was only 29 nm at SS of 1.0 %. The newly formed particles rarely grew larger than 83 nm in size in this NPF event, hence less N_{CCN} enhancement was expected at SS of 0.2 %. In summary, the N_{CCN} enhancement ratios were 1.17–1.88 depending on SS value. In Beijing, a larger N_{CCN} enhancement ratio of 1.4–7 was observed under SS of 0.07–0.86 % caused by NPF (Yue et al., 2011).

In comparison with N_{CCN}, aerosol CCN activity was more sensitive to aerosol size spectra and meteorology factors, which exerts a big complexity into the temporal variation of aerosol activation. Aerosol activities were effectively reduced by abundant ultrafine aerosol particles (CCN-inert) produced during the nucleation period. The minimum (0.2–0.6) of aerosol activities was found at 13:00 LT on April when the particle growth started. Owing to the high survival probability of particles growing from nucleation mode to accumulation mode (CCN size), aerosol activities began to increase at different steps for varying SS and reached their maximums of 0.3–0.9 (0.2–1.0 % SS) at 04:00 LT on 4 April, eight hours after N_{CCN} peaked.

3.2.4   Towards CCN closure for NPF

A kappa value κ describing particle hygroscopiciy, firstly introduced by Petters and Kreidenweis (2007), was employed here to get CCN closure study during NPF. Assuming aerosol particle population is totally internal-mixed, the effective integrated κ can

Title Page

Abstract   Introduction

Conclusions   References

Tables   Figures

◄   ►►

◄   ►

Back   Close

Full Screen / Esc

Printer-friendly Version

Interactive Discussion

be obtained through weighting their chemical compound volume factions,

$$\kappa = \sum_i \varepsilon_i \kappa_i \tag{1}$$

where ε_i is the volume fraction of chemical compounds in particles, and κ_i is the ef-
fective κ of individual chemical composition. This equation has been widely used and
described in detail elsewhere (Petters and and Kreidenweis, 2008; Yue et al., 2011).
In this study, aerosol particle compositions were classified into three categories, and
κ_i and ε_i for individual composition are listed in Table 2, of which "others" refers to
$PM_{2.5} - (SO_4^{2-} + NO_3^- + NH_4^+ + Cl^- + Na^+)$, and is viewed as a chemical compound with
$\kappa_i = 0$ (Yue et al., 2011). As a result, in total, 83.2 % of the effective κ was explained by
$SO_4^{2-} + NO_3^- + NH_4^+$, with their individual contributions of 37.4, 27.5 and 18.3 %, respec-
tively. The critical dry diameter for a particle to act as CCN at a SS can be determined
from an extended κ-Köhler theory, and the relevant Eq. (2) can be found in Petters and
Kreidenweis (2007).

$$S(D) = \frac{D^3 - D_d^3}{D^3 - D_d^3(1 - \kappa)} \exp\left(\frac{4\sigma_{s/a} M_\omega}{RT\rho_\omega D}\right) \tag{2}$$

where ρ_ω is the density of water, M_ω is the molecular weight of water, $\sigma_{s/a}$ is the surface
tension of the solution/air interface, R is the universal gas constant, κ is the hygroscop-
icity parameter, T is temperature, D is the diameter of the droplet and $S(D)$ is the
critical dry size under a given SS. The CCN population can be effectively viewed as
a subset of measured aerosol size distributions since the operating range includes the
majority of atmospheric particles (10–800 nm). Computed for $\sigma_{s/a} = 0.072\,\mathrm{J\,m^{-2}}$ and
$T = 298.15$ K, the predicted CCN number concentration can be calculated through in-
tegration between the bottom and top critical dry diameters.

Figure 10 provides correlation analysis for the hourly-averaged ($N = 70$) predicted
and measured N_{CCN} at SS of 0.2–1.0 %. The agreement was excellent between the

predicted and measured N_{CCN}, and a linear regression produced a slope of 0.98 and an intercept of $-150 \, cm^{-3}$, with a correlation coefficient (R^2) of 0.96. The ratio of $N_{predicted}/N_{measured}$ varied between 0.83 and 1.28 with an average of 1.04.

4 Conclusions

The new particle formation (NPF) events and their impacts on the abundance and properties of cloud condensation nuclei (CCN) were investigated using 1 month continuous measurements collected in downtown Shanghai from 1 to 30 April 2012. The NPF events were observed in 8 out of the 30 days, and their formation and growth rates were $0.60 \, cm^{-3} \, s^{-1}$ and $4.91 \, nm \, h^{-1}$ on average, respectively. The growth rate is important in controlling the conversion of newly formed particles in NPF to possible CCN, whereas the formation rate is viewed as an effective factor only at higher SS (e.g. 1.0 %). This is due to the small critical dry diameters for particles to act as CCN under high SS conditions.

The NPF event on 3 April 2012 showed that aerosol particle enhancement in number concentration significantly relates to the length of nucleation period of NPF, and aerosol particle enhancement in mass concentration depends on the growth period. The nucleation period leads to increased N_{CN} and reduced aerosol activity, while the increases in N_{CCN} and aerosol activity occurred during the growth period. The newly formed particles needed enough time to grow into CCN size and thus N_{CCN} had a delayed peak compared to N_{CN}.

Closure between the measured and predicted N_{CCN} is successful during the NPF event ($R^2 = 0.96$). $SO_4^{2-} + NO_3^- + NH_4^+$ explained the majority of the effective κ, and minimized the impact of lacking organic matter. An overestimation of 4 % for N_{CCN} is probably introduced by the following uncertainties: (1) aerosol assumed to be completely internal-mixed, which is an unrealistic condition and hardly realized in real atmosphere, (2) errors introduced by κ_i for individual chemical composition, and (3) the category "others" typically includes organic carbon (OC), elemental carbon (EC), hy-

drophobic inorganic and other species. Among these other species there are water soluble species contributing to CCN formation. For example, OC has an effective κ value of roughly 0.1 and has been reported to be an important contributor to particle condensational growth. The reasonable closure identified in this study implies that the detailed information of particle size spectra can build an effective CCN prediction model, and size plays a dominant role in aerosol activity during NPF.

It should be noted that the contribution of NPF to CCN has not been fully characterized in this study. For example, the loss of nucleation mode particles by coagulation and the impact of atmospheric dilution and boundary layer evolution on pre-existing and newly formed CCN are unknown. To fully determine NPF contribution to CCN, additional information on size-resolved aerosol composition, size spectra for 3 nm or smaller particles, atmospheric sink and physicochemical process will be needed.

References

Asmi, A., Wiedensohler, A., Laj, P., Fjaeraa, A.-M., Sellegri, K., Birmili, W., Weingartner, E., Baltensperger, U., Zdimal, V., Zikova, N., Putaud, J.-P., Marinoni, A., Tunved, P., Hansson, H.-C., Fiebig, M., Kivekäs, N., Lihavainen, H., Asmi, E., Ulevicius, V., Aalto, P. P., Swietlicki, E., Kristensson, A., Mihalopoulos, N., Kalivitis, N., Kalapov, I., Kiss, G., de Leeuw, G., Henzing, B., Harrison, R. M., Beddows, D., O'Dowd, C., Jennings, S. G., Flentje, H., Weinhold, K., Meinhardt, F., Ries, L., and Kulmala, M.: Number size distributions and seasonality of submicron

particles in Europe 2008–2009, Atmos. Chem. Phys., 11, 5505–5538, doi:10.5194/acp-11-5505-2011, 2011.

Benson, D. R., Yu, J. H., Markovich, A., and Lee, S.-H.: Ternary homogeneous nucleation of H_2SO_4, NH_3, and H_2O under conditions relevant to the lower troposphere, Atmos. Chem. Phys., 11, 4755–4766, doi:10.5194/acp-11-4755-2011, 2011.

Birmili, W. and Wiedensohler, A.: New particle formation in the continental boundary layer: meteorological and gas phase parameter influence, Geophys. Res. Lett., 27, 3325–3328, doi:10.1029/1999GL011221, 2000.

Carslaw, K. S., Spracklen, D. S., Kulmala, M., Kerminen, V. M., Sihto, S. L., and Riipinen, I.: The impact of boundary layer nucleation on global CCN, Aip. Conf. Proc., 911–915, 2007.

Cheng, T. T., Han, Z. W., Zhang, R. J., Du, H. H., Jia, X., Wang, J. J., and Yao, J. Y.: Black carbon in a continental semi-arid area of Northeast China and its possible sources of fire emission, J. Geophys. Res., 115, D23204, doi:10.1029/2009JD013523, 2010.

Cheng, Y., Lee, S. C., Ho, K. F., Wang, Y. Q., Cao, J. J., Chow, J. C., and Watson, J. G.: Black carbon measurement in a coastal area of south China, J. Geophys. Res., 111, D12310, doi:10.1029/2005JD006663, 2006.

Draxler, R. R. and Rolph, G. D.: HYSPLIT (Hybrid Single-Particle Lagrangian Integrated Trajectory) Model access via NOAA ARL READY Website, available at: http://www.arl.noaa.gov/ready/hysplit4.htm, NOAA Air Resources Laboratory, Silver Spring, MD, 2003.

Du, H. H., Kong, L. D., Cheng, T. T., Chen, J. M., Du, J. F., Li, L., Xia, X., Leng. C. P., and Huang, G. H.: Insights into summertime haze pollution events over Shanghai based on online water-soluble ionic composition of aerosols, Atmos. Environ., 45, 5131–5137, 2011.

Du, J. F., Cheng, T. T., Zhang, M., Chen, J. M., He, Q. S.,Wang, X. M., Zhang, R. J., Tao, J., Huang, G. H., Li, X., and Zha, S. P.: Aerosol size spectra and particle formation events at urban Shanghai in eastern China, Aerosol Air Qual. Res., 12, 1362–1372, 2012.

Dumka, U. C., Krishna Moorthy, K., Kumar, R., Hegde, P., Sagar, R., Pant, P., Singh, N., and Suresh Babu, S.: Characteristics of aerosol black carbon mass concentration over a high altitude location in the Central Himalayas from multi-year measurements, Atmos. Res., 96, 510–521, 2010.

Ehn, M., Thornton, J. A., Kleist, E., Sipilä, M., Juuninen, H., Pullinen, L., Springer, M., Rubach, F., Tillmann, R., Lee, B., Lopez-Hilfiker, F., Andres, S., Acir, I.-H., Rissanen, M., Jokinen, T., Schobesberger, S., Kangasluoma, J., Kontkanen, J., Nieminen, T., Kurtén, T., Nielsen, L. B., Jørgensen, S., Kjaergaard, H. G., Canagaratna, M., Maso, M. D., Berndt, T.,

Petäjä, T., Wahner, A., Kerminen, V.-M., Kulmala, M., Worsnop, D. R., Wildt, J., and Mentel., T. F.: A large source of low-volatility secondary organic aerosol, Nature, 506, 476–479, 2014.

Gaydos, T. M., Stanier, C. O., and Pandis, S. N.: Modeling of in situ ultrafine atmospheric particle formation in the eastern United States, J. Geophys. Res., 110, D07S12, doi:10.1029/2004JD004683, 2005.

Ghan, S. J., Easter, R. C., Chapman, E. G., Abdul-Razzak, H., Zhang, Y., Leung, L. R., Laulainen, N. S., Saylor, R. D., and Zaveri, R. A.: A physically based estimate of radiative forcing by anthropogenic sulfate aerosol, J. Geophys. Res., 106, 5279–5293, 2001.

Hansen, A. D. A., Rosen, H., and Novakov, T.: The aethalometer-an instrument for the real-time measurement of optical absorption by aerosol particles, Sci. Total Environ., 36, 191–196, 1984.

Hennigan, C. J., Westervelt, D. M., Riipinen, I., Engelhart, G. J., Lee, T., Collett, J. L., Pandis, S. N., Adams, P. J., and Robinson, A. L.: New particle formation and growth in biomass burning plumes: an important source of cloud condensation nuclei, Geophys. Res. Lett., 39, L09805, doi:10.1029/2012GL050930, 2012.

Hildebrandt, R. L., Smith, J., Riipinen, I., Barsanti, K., Fry, J., Yli-Juuti, T., Petaja, T., Kulmala, M., and McMurry, P. H.: The role of nitrate in the formation of atmospheric nanoparticlers: insights from ambient measurements and chemical transport models, (611f) Environmental division, American Institute of Chemical Engineers Annual Meeting, Pittsburgh, PA, 1 November 2012, 2012.

Hudson J. G. and Noble, S.: CCN and vertical velocity influences on droplet concentration and supersaturations in clean and polluted stratus clouds, J. Atmos. Sci., 106, 24119–24126, 2014.

IPCC: Climate Change 2013: The Physical Science Basis. Contribution of Working Group I to the Fifth Assessment Report of the Intergovernmental Panel on Climate Change, edited by: Joussaume, S., Penner, J., and Tangang, F., IPCC, Stockholm, 2013.

Kerminen, V.-M.: How significantly does coagulation scavenging limit atmospheric particle production?, J. Geophys. Res., 106, 24119–24126, 2001.

Kerminen, V.-M., Lihabainen, H., Lomppula, M., Viisanen, Y., and Kulmala, M.: Direct observational evidence linking atmospheric aerosol formation and cloud droplet activation, Geophys. Res. Lett., 32, L14803, doi:10.1029/2005GL023130, 2005.

Impacts of new particle formation on aerosol CCN

C. Leng et al.

Title Page

Abstract | Introduction

Conclusions | References

Tables | Figures

|◄ | ►|

◄ | ►

Back | Close

Full Screen / Esc

Printer-friendly Version

Interactive Discussion

Kerminen, V.-M., Paramonov, M., Anttila, T., Riipinen, I., Fountoukis, C., Korhonen, H., Asmi, E., Laakso, L., Lihavainen, H., Swietlicki, E., Svenningsson, B., Asmi, A., Pandis, S. N., Kulmala, M., and Petäjä, T.: Cloud condensation nuclei production associated with atmospheric nucleation: a synthesis based on existing literature and new results, Atmos. Chem. Phys., 12, 12037–12059, doi:10.5194/acp-12-12037-2012, 2012.

Köhler, H.: The nucleus in and the the growth of hygroscopic droplets, T. Faraday Soc., 32, 1152–1161, 1936.

Kulmala, M., Laakso, L., Lehtinen, K. E. J., Riipinen, I., Dal Maso, M., Anttila, T., Kerminen, V.-M., Hõrrak, U., Vana, M., and Tammet, H.: Initial steps of aerosol growth, Atmos. Chem. Phys., 4, 2553–2560, doi:10.5194/acp-4-2553-2004, 2004.

Kulmala, M., Petäjä, T., Nieminen, T., Sipilä, M., Manninen, H. E., Lehtipato, K., Dal Maso, M., Aalto, P. P., Junninen, H., Paasonen, P., Riipinen, I., Lehtinen, K. E., Laaksonen, A., and Kerminen, V. M.: Measurement of the nucleation of atmospheric aerosol particles, Nat. Prodoc. 7, 1651–1667, 2012.

Kulmala, M., Kontkanen, J., Junninen, H., Lehtipalo, K., Manninen, H. E., Nieminen, T., Petäjä, T., Sipilä, M., Schobesberger, S., Rantala, P., Franchin, A., Jokinen, T., Järvinen, E., Äijälä, M., Kangasluoma, J., Hakala, J., Aalto, P. P., Paasonen, P., Mikkilä, J., Vanhanen, J., Aalto, J., Hakola, H., Aakkonen, U., Ruuskanen, T., Mauldin III, R. L., Duplissy, J., Vehkamäki, H., Bäck, J., Kortelainen, A., Riipinen, L., Kurtén, T., Johnston, M. V., Smith, J. N., Ehn, M., Mentel, T. F., Lehtinen, K. E. J., Laaksonen, A., Kerminen, V.-M., and Worsnop, D. R.: Direct observations of atmospheric aerosol nucleation, Science, 339, 943–946, 2013.

Kuwata, M. and Kondo, Y.: Dependence of size-resolved CCN spectra on the mixing state of nonvolatile cores observed in Tokyo, J. Geophys. Res., 113, D19202, doi:10.1029/2007JD009761, 2008.

Laakso, L., Merikanto, J., Vakkari, V., Laakso, H., Kulmala, M., Molefe, M., Kgabi, N., Mabaso, D., Carslaw, K. S., Spracklen, D. V., Lee, L. A., Reddington, C. L., and Kerminen, V.-M.: Boundary layer nucleation as a source of new CCN in savannah environment, Atmos. Chem. Phys., 13, 1957–1972, doi:10.5194/acp-13-1957-2013, 2013.

Laaksonen, A., Hamed, A., Joutsensaari, J., Hiltunen, L., Cavalli, F., Junkermann, W., Asmi, A., Fuzzi, S., and Facchini, M. C.: Cloud condensation nucleus production from nucleation events at a highly polluted region, Geophys. Res. Lett., 32, L06812, doi:10.1029/2004GL022092, 2005.

Lance, S., Medina, J., Smith, J. N., and Nenes, A.: Mapping the operation of the DMT Continuous Flow CCN counter, Aerosol Sci. Tech., 40, 242–254, 2006.

Leng, C. P., Cheng, T. T., Chen, J. M., Zhang, R. J., Tao, J., Huang, G. H., Zha, S. P., Zhang, M. G., Fang, W., Li, X., and Li, L.: Measssurements of surface cloud condensation nuclei and aerosol activity in downtown Shanghai, Atmos. Environ., 69, 354–361, 2013.

Lihavainen, H., Kerminen, V. M., Komppula, M., Hatakka, J., Aaltonen, V., Kulmala, M., and Viisanen, Y.: Production of "potential" cloud condensation nuclei associated with atmospheric new particle formation in north Finland, J. Geophys. Res., 108, 4872, doi:10.1029/2003JD003887, 2003.

Lohmann, U. and Feichter, J.: Global indirect aerosol effects: a review, Atmos. Chem. Phys., 5, 715–737, doi:10.5194/acp-5-715-2005, 2005.

McMurry, P. H., Takano, H., and Anderson, G. R.: Study of the ammonia (gas)-sulphuric acid (aerosol) reaction rate, Environ. Sci. Technol., 17, 347–352, 1983.

McMurry, P. H., Fink, M., Sakurai, H., Stolzenburg, M. R., Mauldin, R. L., Smith, J., Eisele, F., Moore, K., Sjostedt, S., Tanner, D., Huey, L. G., Nowak, J. B., Edgerton, E., and Voisin, D.: A criterion for new particle formation in the sulfur-rich Atlanta atmosphere, J. Geophys. Res., 110, D22S02, doi:10.1029/2005JD005907, 2005.

Merikanto, J., Spracklen, D. V., Mann, G. W., Pickering, S. J., and Carslaw, K. S.: Impact of nucleation on global CCN, Atmos. Chem. Phys., 9, 8601–8616, doi:10.5194/acp-9-8601-2009, 2009.

Metzger, A., Verheggen, B., Dommen, J., Duplissy, J., Prevot, A. S., Weingartner, E., Riipinen, I., Kulmala, M., Spracklen, D. V., Carslaw, K. S., and Baltensperger, U.: Evidence for the role of organic in aerosol particle formation under atmospheric conditions, P. Natl. Acad. Sci. USA, 107, 6646–6651, 2010.

Mönkkönen, P., Koponen, I. K., Lehtinen, K. E. J., Hämeri, K., Uma, R., and Kulmala, M.: Measurements in a highly polluted Asian mega city: observations of aerosol number size distribution, modal parameters and nucleation events, Atmos. Chem. Phys., 5, 57–66, doi:10.5194/acp-5-57-2005, 2005.

Nieminen, T., Manninen, H. E., Sihto, S. L., Yli-Juuti, T., Mauldin, R. L., Petaja, T., Riipinen, I., Kerminen, V. M., and Kulmala, M.: Connection of sulfuric acid to atmospheric nucleation in boreal forest, Environ. Sci. Technol., 43, 4715–4721, 2009.

O'Dowd, C. D.: Biogenic coastal aerosol production and its influence on aerosol radiative properties, J. Geophys. Res., 106, 1545–1549, 2001.

Smith, J. N., Moore, K. F., McMurry, P. H., and Eisele, F. L.: Atmospheric measurements of sub-20 nm diameter particle chemical composition by thermal desorption chemical ionization mass spectrometry, Aerosol Sci. Tech., 38, 100–110, 2004.

Spracklen, D. V., Carslaw, K. S., Kulmala, M., Kerminen, V.-M., Mann, G. W., and Sihto, S.-L.: The contribution of boundary layer nucleation events to total particle concentrations on regional and global scales, Atmos. Chem. Phys., 6, 5631–5648, doi:10.5194/acp-6-5631-2006, 2006.

Spracklen, D. V., Carslaw, K. S., Kulmala, M., Kerminen, V. M., Sihto, S. L., Riipinen, I., Merikanto, J., Mann, G. W., Chipperfield, M. P., Wiedensohler, A., Birmili, W., and Lihavainen, H.: Contribution of particle formation to global cloud condensation nuclei concentrations, Geophys. Res. Lett., 35, L06808, doi:10.1029/2007GL033038, 2008.

Vuollekoski, H., Kerminen, V. M., Anttila, T., Sihto, S. L., Vana, M., Ehn, M., Korhonen, H., McFiggans, G., O'Dowd, C. D., and Kulmala, M.: Iodine dioxide nucleation simulations in coastal and remote marine environments, J. Geophys. Res., 114, D00206, doi:10.1029/2008JD010713, 2009.

Wang, Y., Zhuang, G. S., Zhang, X. Y., Huang, K., Xu, C., Tang, A. H., Chen, J. M., and An, Z. S.: The ion chemistry, seasonal cycle, and sources of $PM_{2.5}$ TSP aerosol in Shanghai, Atmos. Environ., 40, 2935–2952, 2006.

Wang, Z. B., Hu, M., Wu, Z. J., and Yue, D. L., Reaserch on the formation mechanism of new particles in the atmosphere, Acta Chim. Sinica, 71, 519–527, 2013.

Weber, R. J., Marti, J. J., McMurry, P. H., Eisele, F. L., Tanner, D. J., and Jefferson, A.: Measured atmospheric new particle formation rates: implications for nucleation mechanisms, Chem. Eng. Commun., 151, 53–64, 1996.

Weber, R. J., McMurry, P. H., Mauldin, R. L., Tanner, D. J., Eisele, F. L., Clarke, A. D., and Kapustin, V. N.: New particle formation in the remote troposphere: a comparison of observations at various sites, Geophys. Res. Lett., 26, 307–310, doi:10.1029/1998GL900308, 1999.

Weingartner, E., Saathoff, H., Schnaiter, M., Streit, N., Bitnar, B., and Baltensperger, U.: Absorption of light by soot particles: determination of the absorption coefficient by means of aethalometers, J. Aerosol Sci., 34, 1445–1463, 2003.

Wiedensohler, A., Cheng, Y. F., Nowak, A., Wehner. B., Achtert, P., Berghof, M., Birmili, W., Wu, Z. J., Hu, M., Zhu, T., Takegawa, N., Kita, K., Kondo, Y., Lou, S. R., Hofzumahaus, A., Holland, F., Wahner, A., Gunthe, S. S., Rose, D., Su, H., and Pöschl. U.: Rapid aerosol growth and increase of cloud condensation nucleus activity by secondary aerosol formation

Title Page

Abstract | Introduction

Conclusions | References

Tables | Figures

|◄ | ►|

◄ | ►

Back | Close

Full Screen / Esc

Printer-friendly Version

Interactive Discussion

and condensation: a case study for regional air pollution in northeastern China, Geophys. Res. Lett., 114, D00G08, doi:10.1029/2008JD010884, 2009.

Wu, Z., Hu, M., Liu, S., Wehner, B., Bauer, S., Mäßling, A.Wiedensohler, A., Petäjä, T., Dal Maso, M., and Kulmala, M.: New particle formation in Beijing, China: statistical analysis of a 1-year dataset, J. Geophys. Res., 112, D09209, doi:10.1029/2006JD007406, 2007.

Yu, F. Q.: Effect of ammonia on new particle formation: a kinetic H_2SO_4-H_2O-NH_3 nucleation model constrained by laboratory measurements, J. Geophys. Res., 111, D01204, doi:10.1029/2005JD005968, 2006.

Yu, F., Wang, Z., Luo, G., and Turco, R.: Ion-mediated nucleation as an important global source of tropospheric aerosols, Atmos. Chem. Phys., 8, 2537–2554, doi:10.5194/acp-8-2537-2008, 2008.

Yu, H., McGraw, R., and Lee, S. H.: Effects of amines on formation of sub-3 nm particles and their subsequent growth, Geophys. Res. Lett., 39, L02807, doi:10.1029/2011GL050099, 2012.

Yue. D. L., Hu. M., Zhang. R. J., Wu. Z. J., Su. H., Wang, Z. B., Peng, J. F., He, L. Y., Huang, X. F., Gong, Y. G., and Wiedensohler, A.: Potential contribution of new particle formation to cloud condensation nuclei in Beijing, Atmos. Environ., 45, 6070–6077, 2011.

Zhang, R., Jing, J., Tao, J., Hsu, S.-C., Wang, G., Cao, J., Lee, C. S. L., Zhu, L., Chen, Z., Zhao, Y., and Shen, Z.: Chemical characterization and source apportionment of $PM_{2.5}$ in Beijing: seasonal perspective, Atmos. Chem. Phys., 13, 7053–7074, doi:10.5194/acp-13-7053-2013, 2013.

Zhang, R. Y.: Getting to the critical nucleus of aerosol formation, Science, 328, 1366–1367, 2010.

Zhang, R. Y., Khalizov, A., Wang, L., Hu, M., and Xu, W.: Nucleation and growth of nanoparticles in the atmosphere, Chem. Rev., 112, 1957–2011, 2012.

Zheng, J., Hu, M., Zhang, R., Yue, D., Wang, Z., Guo, S., Li, X., Bohn, B., Shao, M., He, L., Huang, X., Wiedensohler, A., and Zhu, T.: Measurements of gaseous H_2SO_4 by AP-ID-CIMS during CAREBeijing 2008 Campaign, Atmos. Chem. Phys., 11, 7755–7765, doi:10.5194/acp-11-7755-2011, 2011.

Title Page

Abstract | Introduction

Conclusions | References

Tables | Figures

|◀ | ▶|

◀ | ▶

Back | Close

Full Screen / Esc

Printer-friendly Version

Interactive Discussion

Table 1. Comparison of CCN enhancement ratios from NPF events with different FR and GR.

	0.2 %	0.4 %	0.6 %	0.8 %	1.0 %
Enhancement ratio (FR > 0.40)	1.18	1.84	1.88	1.84	1.77
Enhancement ratio (FR < 0.40)	1.15	1.89	1.81	1.77	1.58
Enhancement ratio (GR > 4.91)	1.25	1.95	2.03	1.93	1.72
Enhancement ratio (GR < 4.91)	1.10	1.79	1.80	1.74	1.63

Table 2. Effective hygroscopicity parameters (κ) and densities of the four category compositions.

Species	Data source	κ	Density (g cm^{-3})
Sulfate and nitrate	$SO_4^{2-} + NO_3^- + NH_4^+$	0.6	1.7
Sodium chloride	$Cl^- + Na^+$	1	2.2
Insoluble compounds	Others	0	2.0
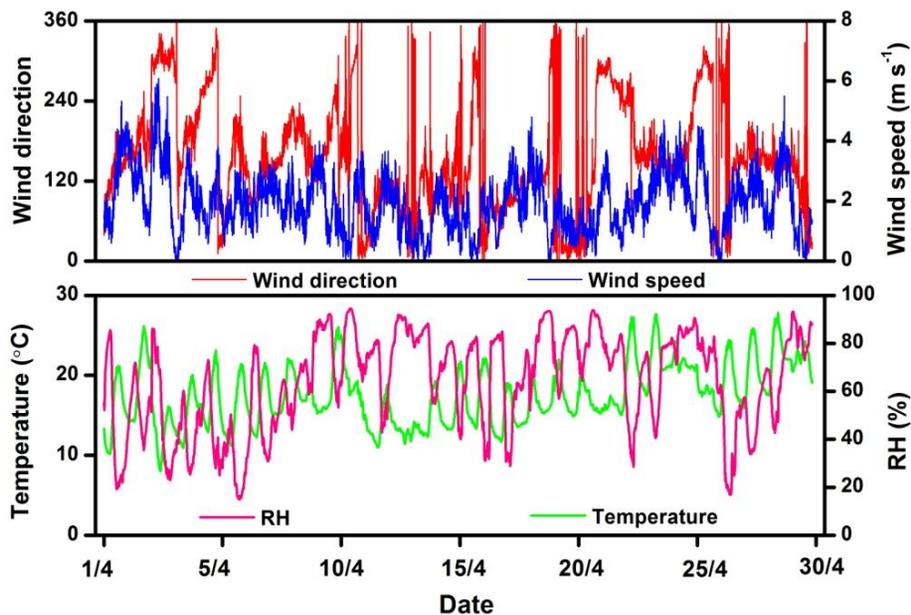
Figure 1. Series of 10 min mean meteorological parameters over the entire campaign.
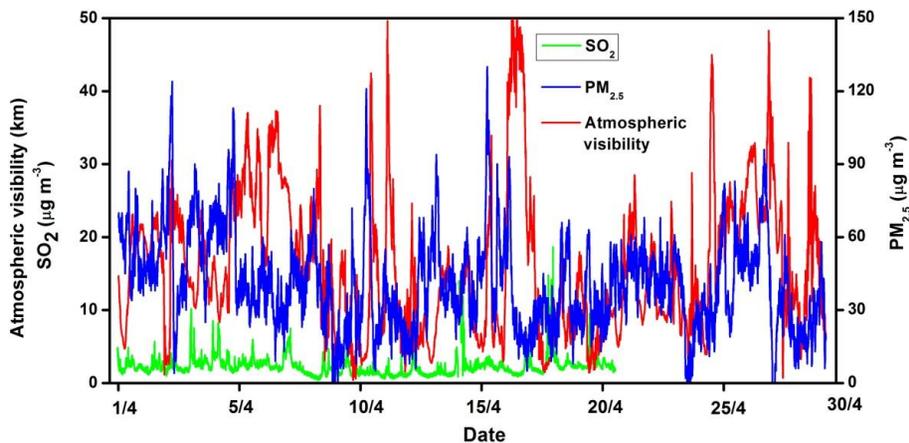
Figure 2. Series of 5 min mean SO_2 and $PM_{2.5}$ concentration and atmospheric visibility over the entire campaign.
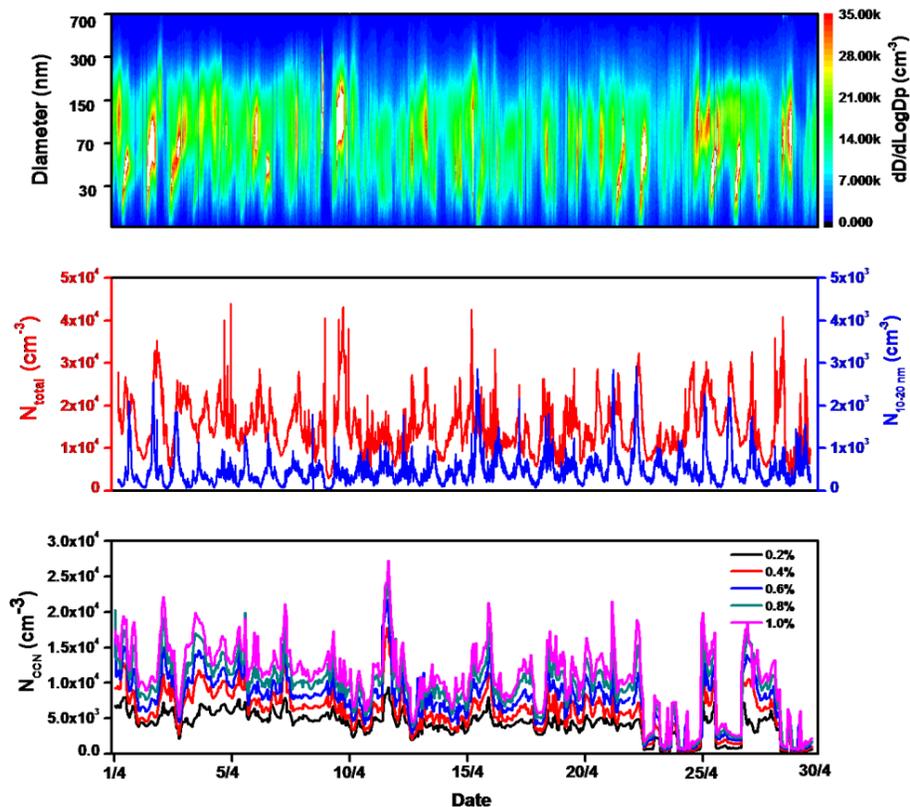
Figure 3. Series of aerosol size distribution, 5 min mean total (N_{total}) and nucleation ($N_{10-20\,\text{nm}}$) mode aerosol number concentration and 1 h mean CCN concentration over the entire campaign.

Figure 4. Temporal evolution of aerosol size spectra, showing new particle formation and subsequent growth on 3 and 4 April 2012.
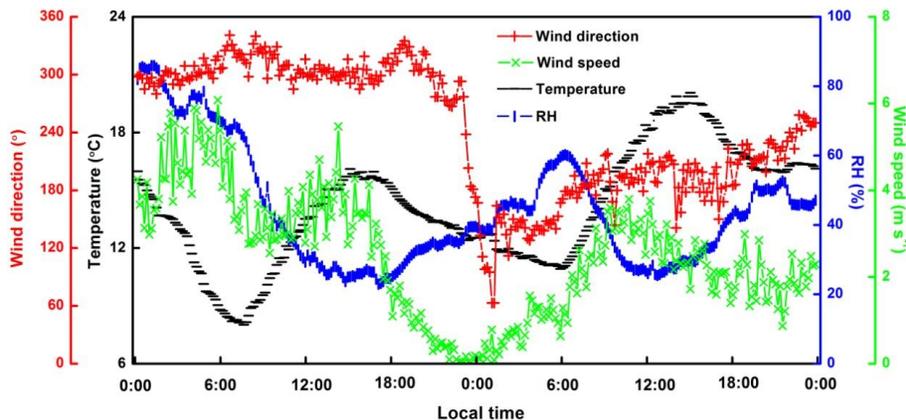
Figure 5. Temporal evolution of main meteorological parameters during the new particle formation event on 3–4 April 2012.
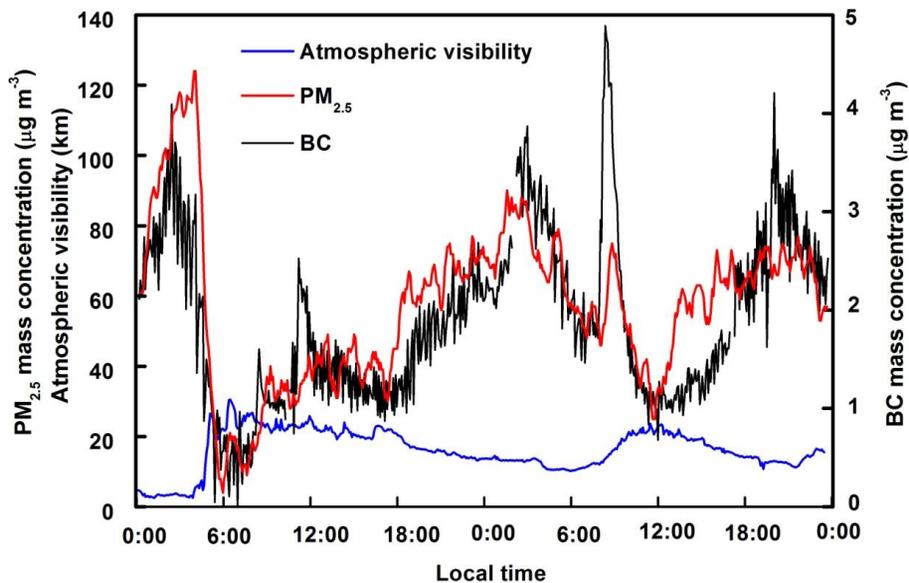
Figure 6. Temporal evolutions of total aerosol number (CN), BC and PM$_{2.5}$ concentrations during the new particle formation event on 3–4 April 2012.
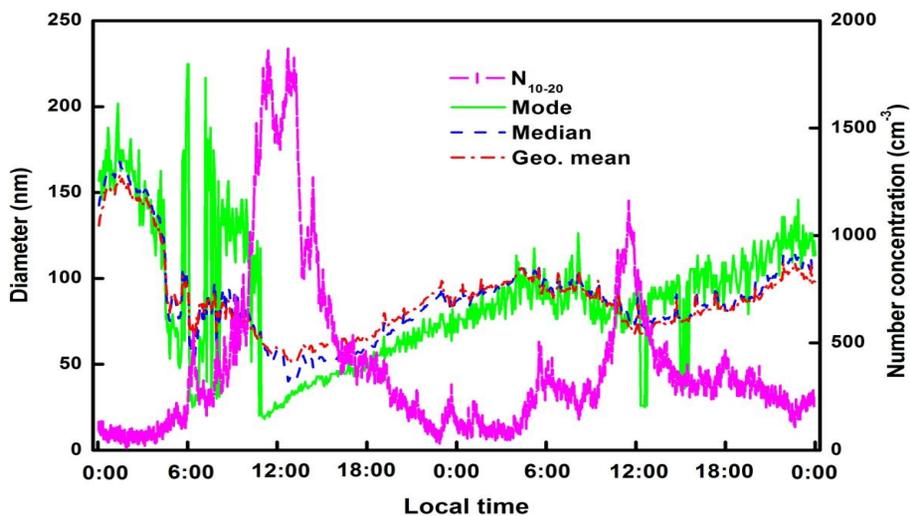
Figure 7. Temporal evolutions of mode, median and diameters and 10–20 nm particle concentration, showing the growth rate and formation of new particle on 3–4 April 2012.
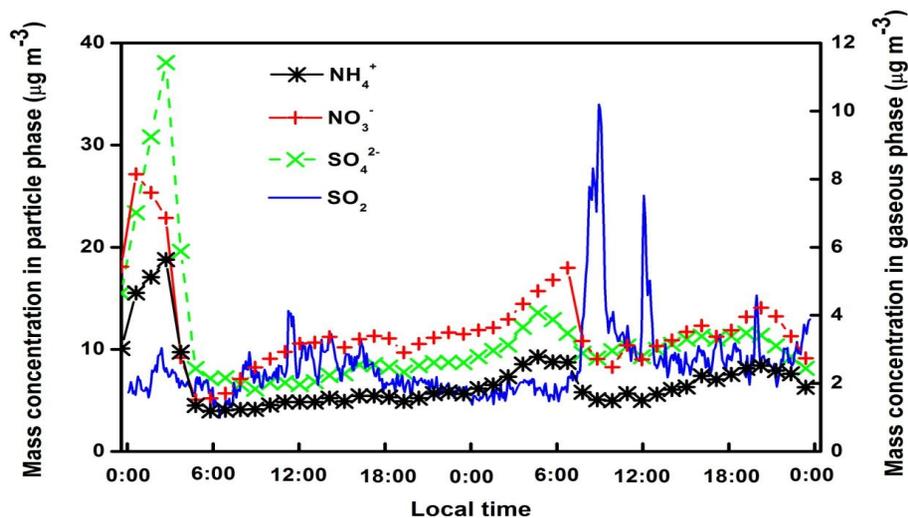
Figure 8. Series of SO_2, SO_4^{2-}, NO_3^- and NH_4^+ concentrations on 3 and 4 April 2012.

Figure 9. Series of CCN concentration and CCN/CN on 3 and 4 April 2012.
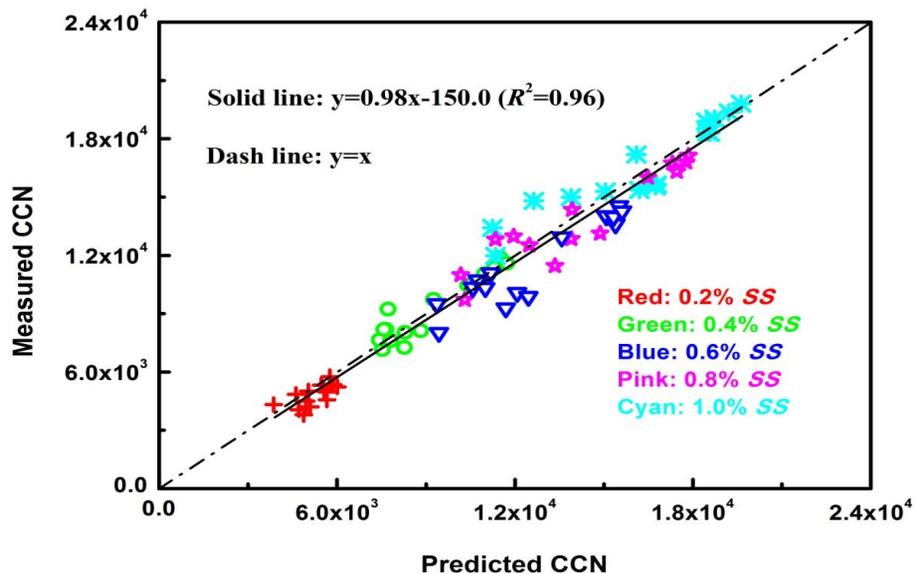
Figure 10. Scatterplots of predicted and measured CCN concentrations at different SS conditions, the red dash line represents $y = x$.